



HAL
open science

Turbulent vertical diffusivity in the sub-tropical stratosphere

I. Pisso, B. Legras

► **To cite this version:**

I. Pisso, B. Legras. Turbulent vertical diffusivity in the sub-tropical stratosphere. *Atmospheric Chemistry and Physics Discussions*, 2007, 7 (3), pp.6603-6629. hal-00328083

HAL Id: hal-00328083

<https://hal.science/hal-00328083>

Submitted on 18 Jun 2008

HAL is a multi-disciplinary open access archive for the deposit and dissemination of scientific research documents, whether they are published or not. The documents may come from teaching and research institutions in France or abroad, or from public or private research centers.

L'archive ouverte pluridisciplinaire **HAL**, est destinée au dépôt et à la diffusion de documents scientifiques de niveau recherche, publiés ou non, émanant des établissements d'enseignement et de recherche français ou étrangers, des laboratoires publics ou privés.

**Turbulent vertical
diffusivity in the
sub-tropical
stratosphere**

I. Pisso and B. Legras

Turbulent vertical diffusivity in the sub-tropical stratosphere

I. Pisso and B. Legras

Laboratoire de Meteorologie Dynamique UMR 8539, Paris, France

Received: 14 March 2007 – Accepted: 26 March 2007 – Published: 16 May 2007

Correspondence to: I. Pisso (ipisso@lmd.ens.fr)

Title Page

Abstract

Introduction

Conclusions

References

Tables

Figures

⏪

⏩

◀

▶

Back

Close

Full Screen / Esc

Printer-friendly Version

Interactive Discussion

Abstract

Vertical (cross-isentropic) mixing is produced by small-scale turbulent processes which are still poorly understood and parametrized in numerical models. In this work we provide estimates of local equivalent diffusion in the lower stratosphere by comparing balloon borne high-resolution measurements of chemical tracers with reconstructed mixing ratio from large ensembles of random Lagrangian backward trajectories using European Center for Medium-range Weather Forecasts analysed winds and a chemistry-transport model (REPROBUS). We have investigated cases in subtropical latitudes using data from HIBISCUS campaign. Upper bound on the vertical diffusivity is found to be of the order of $0.5 \text{ m}^2 \text{ s}^{-1}$ in the subtropical region, which is larger than the estimates at higher latitudes. The relation between diffusion and dispersion is studied by estimating Lyapunov exponents and studying their variation according to the presence of active dynamical structures.

1 Introduction

The lower stratosphere can be divided in two parts: an “overworld” region corresponding to the range of potential temperature above the tropical cold point tropopause at about 380 K in potential temperature (θ) and an extra-tropical “lowermost stratosphere” (ETLS) below, sharing a range of θ levels, between 340 K and 380 K, with the tropical upper troposphere also called Tropical Tropopause Layer (TTL) (Highwood and Hoskins, 1998)

The TTL is separated from the ETLS by the subtropical jets centered in both hemispheres at 200 hPa in pressure or 350 K in potential temperature. These jets are partial transport barriers to isentropic motion (Del Castillo-Negrete and Morrison, 1993; Haynes and Shuckburgh, 2000) explaining the observed gradient of long-lived tracers and potential vorticity across them.

Rossby waves are, however, modulating these jets and are capable to generate

Turbulent vertical diffusivity in the sub-tropical stratosphere

I. Pisso and B. Legras

Title Page

Abstract

Introduction

Conclusions

References

Tables

Figures

⏪

⏩

◀

▶

Back

Close

Full Screen / Esc

Printer-friendly Version

Interactive Discussion

**Turbulent vertical
diffusivity in the
sub-tropical
stratosphere**

I. Pisso and B. Legras

Title Page

Abstract

Introduction

Conclusions

References

Tables

Figures

⏪

⏩

◀

▶

Back

Close

Full Screen / Esc

Printer-friendly Version

Interactive Discussion

tropical intrusions of TTL air in the mid-latitudes ETLS and, conversely, intrusions of ETLS air, rich in ozone and poor in tropospheric tracers, within the tropical region. Such events transport air masses with mixing ratios of trace gases typical of high latitudes from the lowermost stratosphere into the TTL (Waugh and Polvani, 2000) influencing the chemical composition of the tropical reservoir. This two way stratosphere-troposphere exchange coupling the upper troposphere with the lowermost stratosphere (LMS) is a key controlling process for the upper tropospheric ozone budget (Holton et al., 1995) and climate simulations (Sudo et al., 2003).

In the “overworld” lower stratosphere, global observations from space and airborne experiments show that many chemical species have different tropical and extra-tropical mixing ratios along a same isentropic surface and present steep tracer gradients at the edges of the “tropical pipe” (McCormick and Veiga, 1992; Waugh et al., 1994; Waugh, 1996; Neu and Plumb, 1999). It should be noted that this overworld barrier is separated from the subtropical jet barrier by a region above the tropopause near $\theta=400$ K where meridional exchanges are more favored (Waugh, 1996).

Transport barriers are, however, not impermeable and meridional exchanges occur due to breaking Rossby waves that generate intrusions. This dynamics induces, by chaotic transport, a number of small-scale structures and heterogeneities (Pierrehumbert and Yang, 1993) which have an impact on the composition of the atmosphere and its radiative properties. Although such mechanisms are fairly well understood and can be described with analysed winds, the amount of net irreversible exchange, which requires not only transport but also mixing of air masses, is still poorly understood and not well represented in meteorological models. Irreversibility results from small-scale turbulent mixing, either due to shear instabilities, convection or gravity wave breaking, occurring at scales too small to be represented in numerical models.

General circulation models and chemistry-transport models (CTM) include numerical diffusion that attempts to represent such effects but this has to be too large due to limited resolution. It is therefore interesting to investigate the natural value of diffusion induced by subgrid scale processes. Such estimates have been provided by

comparing Lagrangian calculations with observed distributions of tracers at high and mid-latitudes (Balluch and Haynes, 1997; Legras et al., 2005), reaching estimates in the range $D=0.01-0.1\text{ m}^2\text{ s}^{-1}$, but no study of the subtropical region has been performed so far.

In this work estimates of local equivalent diffusion in the lower stratosphere are provided by comparing balloon borne high-resolution measurements of chemical tracers with reconstructed mixing ratio from large ensembles of stochastic Lagrangian backward trajectories using the European Center for Medium range Weather Forecast (ECMWF) analysed wind fields and outputs from the REPROBUS (REactive Processes Ruling the Ozone BUDget in the Stratosphere) chemistry-transport model. We will focus on the cases of intrusions detected during the Hibiscus campaign above 15 km.

The measurements collected during Hibiscus tropical campaign and the methods used for analysis are presented in Sect. 2. In Sect. 3, the skill of ensembles of diffusive back trajectories to model transport in the tropics is studied, focusing on the ability to represent synoptic structures related to intrusions. Based on the Lagrangian reconstructions of O_3 profiles from the Hibiscus campaign, the magnitude of turbulent diffusivity in the tropics is estimated. Results are discussed and conclusions are presented in Sect. 4.

2 Data and methods

2.1 The Hibiscus campaign

During the Hibiscus campaign (Pommereau et al., 2007), SF balloon flights carried a Solid State Ozone Sensor instrument (Hansford et al., 2005; Aliwell et al., 2001; Williams et al., 2002). The sensor was developed by the University of Cambridge, and consists of a thin metal oxide (tungsten oxide) layer mounted on a small ($2\text{ mm}\times 2\text{ mm}$) ceramic tile. Typical time response of the device is in the order of a few seconds (Pommereau et al., 2007). Sampling frequency is about 1 Hz, yielding about 10 000

Turbulent vertical diffusivity in the sub-tropical stratosphere

I. Pisso and B. Legras

Title Page

Abstract

Introduction

Conclusions

References

Tables

Figures

◀

▶

◀

▶

Back

Close

Full Screen / Esc

Printer-friendly Version

Interactive Discussion

measurement points per flight, with an effective resolution of about 0.2 Hz. These measurements are compared to those collected by the DMI flights (Pommereau et al., 2007) carrying an ozone sonde (Electro Chemical Cell) from Danish Meteorological Institute which reached a mean altitude of 35 km, with a lower resolution. In this study, we focus on the O₃ profiles collected during two SF flights.

The first flight considered in this study is the SF2 flight launched on 13 February 2004 under a meteorological situation shown in Fig. 1 where a fresh large intrusion of extratropical air was sitting above the launching site of Bauru (Brazil). The three O₃ profiles shown in the first panel of Fig. 2 were collected during the ascent and descent phases of the SF2 flight and during the DMI flight launched the same day, and exhibit clearly defined structures appearing as peaks in the mixing ratio curves. In the same panel are drawn the temperature profiles collected by SF2 at the same time showing almost no difference between ascent and descent and in both cases a temperature inversion located in the same layer as the O₃ peak. The second panel in Fig. 2, shows the water vapor profile collected during the descent, and exhibits an absolute minimum correlated with the O₃ peak of the descent profile. The third panel shows the CH₄ profile collected during the ascent and exhibits an absolute minimum around 17 km that coincides with the O₃ peak of the ascent phase. The large values of O₃ mixing ratio in the peaks with respect to the background values and the low values in water vapor and CH₄ suggest the presence of a layer of extra-tropical intrusion.

SF1 was launched three days later, on 16 February, while the intrusion had ended but left significant remains of extra tropical air in the region surrounding Bauru as suggested by the meteorological situation shown in Fig. 1. Figure 3 shows O₃ mixing ratio profiles collected during the ascent and descent phases of SF1 flight and during the ascent of DMI flight launched at 00:08 UT the same day. The three O₃ profiles show peaks in mixing ratio values at different altitudes between 17.5 and 18 km. The SF1 ascent profile shows the peak shifted down with respect to the SF1 descent profile, and the in the DMI profile is even lower. The temperature collected during SF1 ascent and descent is also drawn showing almost no difference between ascent and descent

Turbulent vertical diffusivity in the sub-tropical stratosphereI. Pisso and B. Legras

Title Page

Abstract

Introduction

Conclusions

References

Tables

Figures

⏪

⏩

◀

▶

Back

Close

Full Screen / Esc

Printer-friendly Version

Interactive Discussion

Turbulent vertical diffusivity in the sub-tropical stratosphere

I. Pisso and B. Legras

Title Page

Abstract

Introduction

Conclusions

References

Tables

Figures

⏪

⏩

◀

▶

Back

Close

Full Screen / Esc

Printer-friendly Version

Interactive Discussion

and an inversion around 18 km located close to the three O₃ peaks. This suggests a less stable situation than during SF2 flight, with an O₃ rich layer sloping vertically and moving during the day. This is further suggested by Fig. 4 showing the potential temperature as a function of altitude (first panel) and the O₃ mixing ratio as a function of potential temperature. The first shows two inversions under and above 18 km and the latter shows the region of high O₃ as a thick layer of 10 K detected at the same location during ascent and descent for SF2, whereas for SF1 a layer of 5 K is detected only during descent.

2.2 Diffusive backward trajectories

Because the typical horizontal/vertical aspect ratio of tracer structures in the stratosphere is large (Haynes and Anglade, 1997), the main contributor to mixing is the vertical turbulent motion. This motivates the representation of small-scale turbulence in Lagrangian calculations as a vertical stochastic perturbation on the velocity field. The stochastic perturbation takes into account the turbulent motions occurring at unresolved scales. It is assumed that the overall effect of turbulence in a spatial scale smaller than the advecting fields grid has time scales much smaller than the time step of advection and hence can be approximated as a diffusive process. The displacement of an individual particle due to the perturbation and the advecting velocity reads:

$$\delta \mathbf{x} = \mathbf{u}(\mathbf{x}, t) \delta t + \mathbf{k} \delta \eta(t) \quad (1)$$

where \mathbf{k} is the vertical unit vector and $\delta \eta(t) = w(t) \delta t$ is the product of a white noise process $w(t)$ by the time step δt . In this work, independent perturbations are applied to each member of a large ensemble of backward trajectories.

The solution to the advective diffusive equation

$$\frac{\partial C}{\partial t} + \mathbf{u}(\mathbf{x}, t) \cdot \nabla C = D \Delta C \quad (2)$$

for impulsive initial conditions yields that the standard deviation of the positions of a diffused cloud of particles released at time $t=0$ is $\sigma = \sqrt{2Dt}$, where D is the diffusivity.

The random perturbation in Eq. (1) is constructed with a random variable r which is uniform, with zero mean and unit variance, and such that

$$\delta\eta(t) = r\sqrt{2D\delta t}$$

which relates the white noise and the diffusivity D by the equation

$$D = \frac{1}{2} \langle w(t)^2 \rangle \delta t$$

where the average $\langle \rangle$ is taken over the members of an ensemble of particles launched from an individual measure point. This technique is related to the solution to Eq. (2) by the Green function technique to obtain the field caused by a distributed source (i.e. the concentration in a time s previous to t). If $G(\mathbf{x}, t; \mathbf{y}, s)$ is the concentration at the point \mathbf{x} at time t caused by a unit point source at the point \mathbf{y} at time s , then the field at (\mathbf{x}, t) caused by a source distribution $C(\mathbf{y}, s)$ can be described as the integral

$$C(\mathbf{x}, t) = \int G(\mathbf{x}, t; \mathbf{y}, s) C(\mathbf{y}, s) d^3\mathbf{y} \quad (3)$$

where $G(\mathbf{x}, t; \mathbf{y}, s)$ satisfies the two equations (Morse and Feschbach, 1953; Legras et al., 2005):

$$\begin{aligned} \frac{\partial G}{\partial t} + \mathbf{u}(\mathbf{x}, t) \cdot \nabla_{\mathbf{x}} G - \frac{D}{\rho(\mathbf{x}, t)} \nabla_{\mathbf{x}} \rho(\mathbf{x}, t) \nabla_{\mathbf{x}} G \\ = \frac{1}{\rho(\mathbf{y}, s)} \delta(t - s) \delta(\mathbf{y} - \mathbf{x}), \end{aligned} \quad (4)$$

$$\begin{aligned} \frac{\partial G}{\partial s} + \mathbf{u}(\mathbf{y}, s) \cdot \nabla_{\mathbf{y}} G + \frac{D}{\rho(\mathbf{y}, s)} \nabla_{\mathbf{y}} \rho(\mathbf{y}, s) \nabla_{\mathbf{y}} G \\ = -\frac{1}{\rho(\mathbf{x}, t)} \delta(t - s) \delta(\mathbf{y} - \mathbf{x}). \end{aligned} \quad (5)$$

Turbulent vertical diffusivity in the sub-tropical stratosphere

I. Pisso and B. Legras

Title Page

Abstract

Introduction

Conclusions

References

Tables

Figures

⏪

⏩

◀

▶

Back

Close

Full Screen / Esc

Printer-friendly Version

Interactive Discussion

Here the derivatives are taken with respect to the final coordinates x and t for the first equation and with respect to the initial coordinates y and s for the second one. The negative sign in front of the diffusive term on the right hand side of Eq. (5) means that this equation is well-posed for backward integration in time. For a more detailed discussion, see [Holzer and Hall \(2000\)](#); [Issartel and Baverel \(2003\)](#); [Dexheimer and Bowman \(2004\)](#).

2.3 TRACZILLA

Reverse integrations of trajectories initialised along each transect have been performed with TRACZILLA, a modified version of FLEXPART ([Stohl et al., 2005](#)) which uses ECMWF winds at 1° horizontal resolution and on 60 hybrid levels with 3-h resolution obtained by combining analysis available every 6 h with short time forecasts at intermediate times (3 h resolution). The modifications from FLEXPART advection scheme consists mainly in discarding the intermediate terrain following coordinate system and in performing a direct vertical interpolation of winds, linear in log-pressure, from hybrid levels. The vertical velocities used in this work are computed by the FLEXPART pre-processor using a mass conserving scheme in the hybrid ECMWF coordinates. The model uses a fixed time step of $\delta t=900$ s. The release size N of the ensemble of trajectories used in this work is either $N=500$ or $N=2000$. Time lag between particle release is either 1 s or 30 s along the balloon track.

We use the balloon GPS data and the on-board pressure sensor to locate the launching point of each parcel, respectively horizontally and vertically.

2.4 REPROBUS

Chemical mixing ratios were interpolated from REPROBUS 3-D output fields. REPROBUS (REactive Processes Ruling the Ozone BUDget in the Stratosphere) is a three-dimensional chemical-transport model with a comprehensive treatment of gas-phase and heterogeneous chemical processes in the stratosphere ([Lefèvre](#)

Turbulent vertical diffusivity in the sub-tropical stratosphere

I. Pisso and B. Legras

Title Page

Abstract

Introduction

Conclusions

References

Tables

Figures

◀

▶

◀

▶

Back

Close

Full Screen / Esc

Printer-friendly Version

Interactive Discussion

et al., 1994, 1998). Long-lived species, including ozone, are transported by a semi-Lagrangian scheme (Williamson, 1989) forced by the ECMWF wind analysis. The model is integrated on 42 hybrid pressure levels that extend from the ground up to 0.1 hPa, with a horizontal resolution of 2 degrees and a time resolution of 3 h.

3 Results

3.1 SF2 and active intrusion

3.1.1 Back trajectories

In order to study the origin and dynamical history of the sampled air, back-trajectories have been initialised starting from each measure point along SF2 flight track between 15 and 17.5 km above Bauru.

Figure 5a shows the 3-D back trajectories calculated over 9 days before the SF2 flight without added diffusion, and Fig. 5b shows the same set of back trajectories projected onto the latitude-altitude plane. For most of the trajectories, the air comes from regions located north of the launching site and altitudes above 15 km. However, the group of air parcels sampled between 16 and 17 km (in yellow) originate from latitudes below 70 S and altitudes below 14 km. This is consistent with the peak of O₃ mixing ratio measured by SF2 instruments at 17 km and suggests that the mixing ratio peak is due to the layering of an extra-tropical air intrusion across the subtropical barrier.

Figure 6 compares the O₃ reconstruction from this set of non diffusive trajectories with O₃ measurements during SF2 flight. In spite of the very large noise inherent to this reconstruction, we see that the peaks between 15 and 16 km, at 17 km and at 19 km are all associated with bumps in the observed profile. The depleted layer between 17 and 18 km is also seen in the observed profile. All these features are, however, strongly exaggerated in the reconstruction. The upper part of the reconstructed profile, above 18 km tends to follow the REPROBUS profile and to depart from the observations,

Turbulent vertical diffusivity in the sub-tropical stratosphere

I. Pisso and B. Legras

Title Page

Abstract

Introduction

Conclusions

References

Tables

Figures

⏪

⏩

◀

▶

Back

Close

Full Screen / Esc

Printer-friendly Version

Interactive Discussion

resulting in an underestimation of about 50%. We meet here one of the fundamental limitations of reconstructions which is that they are able to regenerate the small scales of the tracer but they depend on the accuracy of the supporting CTM or chemical data for the mean gradients. In fact, REPROBUS underestimates ozone in most of the lower tropical and subtropical stratosphere (G. Berthet, personal communication).

3.1.2 Diffusive reconstructions

In order to estimate the vertical diffusivity coefficient, we compare now the values of O_3 mixing ratio measured by SF2 sonde with diffusive reconstructions with the TRACZILLA model. Figure 7 shows the reconstructions obtained with a range of diffusivity from $D=10^{-3} \text{ m}^2 \text{ s}^{-1}$ to $D=1 \text{ m}^2 \text{ s}^{-1}$. In addition to adding vertical diffusion, we have also filtered the reconstructions with a moving centered mean over 5 s in order to simulate the response function of the instrument (Pommereau et al., 2007).

In the lower layers, corresponding to the troposphere, the mean reconstructed O_3 is closer to the measurements than the prediction of REPROBUS. Small diffusivity $D \leq 0.1 \text{ m}^2 \text{ s}^{-1}$, however, generates a number of fluctuations which are not observed. It is only for $D=0.5 \text{ m}^2 \text{ s}^{-1}$ that the fluctuations are reduced to the level of the observations below 14 km.

Above the tropopause, the peak in O_3 mixing ratio located between 16 and 17 km, corresponding to the extra-tropical intrusion, is reproduced in all reconstructions but overestimated for values of D below $0.1 \text{ m}^2 \text{ s}^{-1}$. The difference with the measured values in this layer is of more than 100% for the values $D=0.001 \text{ m}^2 \text{ s}^{-1}$ and $D=0.01 \text{ m}^2 \text{ s}^{-1}$. However, the slope of the curve, which represents the gradient of mixing ratio, is too steep for $D=0.1 \text{ m}^2 \text{ s}^{-1}$. It is again with $D=0.5 \text{ m}^2 \text{ s}^{-1}$ that we reach the best agreement with the observations both for the peak at 17 km and the depleted layer between 17 and 18 km. The position of the peak is only shifted by 200 m in the reconstruction.

Above 18 km, where REPROBUS departs significantly from the observations, the reconstructions exclude any value less than $0.1 \text{ m}^2 \text{ s}^{-1}$ which produces too large, un-

Turbulent vertical diffusivity in the sub-tropical stratosphere

I. Pisso and B. Legras

Title Page

Abstract

Introduction

Conclusions

References

Tables

Figures

◀

▶

◀

▶

Back

Close

Full Screen / Esc

Printer-friendly Version

Interactive Discussion

observed fluctuations. On the other side, the closeness between observations and $1 \text{ m}^2 \text{ s}^{-1}$ profile is only a spurious result that compensates the underprediction of ozone by REPROBUS by increased diffusion along the vertical gradient. Small wiggles on the reconstructed curve are due to sampling effects which increase with D in the reconstructions.

The profile of the tracer variance within the cloud of points associated with each parcel is also shown in Fig. 7. Lower-right panel shows that, for several values of D , the variance is well correlated with the mean. The fact that $\frac{\sqrt{\langle C'^2 \rangle}}{\langle C \rangle} \approx \text{constant}$ is consistent with fluctuations C' being due to displacements in the vertical and horizontal gradients of C .

3.2 SF1 and decaying intrusion

Figure 1b shows that on 16 February, the active phase of the intrusion dominating on 13 February has ended and the region surrounding Bauru is filled with numerous remains as patches of high PV. This suggests that tracers are also distributed as patches and that lamination might occur over a small area rather than over a broad domain like on 13 February. This suggests also that reconstructions will perform less accurately in that case.

Indeed, diffusive reconstructions with a small value of D of $0.1 \text{ m}^2 \text{ s}^{-1}$, which generally tend to exaggerate features in observed profiles do not show even one hint of the peak of O_3 mixing ratio in the profile of SF1 flight as seen in Fig. 9a.

In order to investigate the causes of this discrepancy, ensembles of diffusive backward trajectories have been initialised not only at measured locations along the balloon track but also at other locations in its neighborhood.

Figure 8 shows a 3-D neighborhood (21 S to 26 S in latitude, 46 W to 52 W in longitude and 85 hPa to 75 hPa in pressure) of the SF1 flight segment over which the peaks were detected. This figure is generated by performing diffusive reconstructions with $D=0.1 \text{ m}^2 \text{ s}^{-1}$ in three horizontal planes at three pressure levels: 85 hPa (17.25 km),

Turbulent vertical diffusivity in the sub-tropical stratosphere

I. Pisso and B. Legras

Title Page

Abstract

Introduction

Conclusions

References

Tables

Figures

⏪

⏩

◀

▶

Back

Close

Full Screen / Esc

Printer-friendly Version

Interactive Discussion

80 hPa (17.65 km, around the maximum of O_3) and 85 hPa (18.15) km respectively. It is clear that Bauru is, according to this map, located in a region with O_3 less than 0.3 ppbv just north of a large meridional gradient in ozone concentration with values of the order of 0.4 ppbv at 200 km from the launch site. The accuracy in the location of such gradient depends both on the chemical initialization field and on the advecting winds. Displacements of the order of tens of kilometers are very common when comparing observed and reconstructed structures along aircraft tracks (Legras et al., 2005, e.g.). It is likely that the missing bump on the SF1 reconstructed profile could be found in the neighborhood of Bauru, on the southern side.

Hence, we have reconstructed the O_3 profile over the 5 profiles along the vertical lines in Fig. 8 distributed horizontally over a segment running between the launch site at (22.5 S, 49.5 W) and (25.85 S, 47.46 W) where reconstructed O_3 is high. The reconstructed profiles in Fig. 9b–f show that a peak of O_3 near 18 km is obtained in panels (d) to (f). This peak is larger than the observed one and is vertically shifted by about 300 m. Different values of D yield different structures in the distribution on O_3 in this region. The determination of a unique value for D relies on the identification and reconstruction of measured tracer structures, and here additional hypothesis are needed to constrain the values of diffusivity. Hence, it is not possible from these reconstructions to estimate D accurately.

3.3 Detecting dynamical boundaries

Regions of high dispersion in the flow (i.e., rapid separation of pairs of particles) are characterized by maxima of Lyapunov exponents (Pierrehumbert and Yang, 1993; Legras et al., 2005). Finite time Lyapunov exponents, which describe the transformation of an infinitesimal spherical cloud surrounding a particle at time t_0 into an ellipsoid at time t_1 in a local reference frame relative to the particle, have been calculated along the balloon tracks in order to study the dynamical history of the sampled air. The calculation of the three local Lyapunov exponents around a deterministic particle trajectory is performed by using a triad of orthogonal displacement around the initial position. Such

Turbulent vertical diffusivity in the sub-tropical stratosphere

I. Pisso and B. Legras

Title Page

Abstract

Introduction

Conclusions

References

Tables

Figures

⏪

⏩

◀

▶

Back

Close

Full Screen / Esc

Printer-friendly Version

Interactive Discussion

**Turbulent vertical
diffusivity in the
sub-tropical
stratosphere**

I. Pisso and B. Legras

Title Page

Abstract

Introduction

Conclusions

References

Tables

Figures

⏪

⏩

◀

▶

Back

Close

Full Screen / Esc

Printer-friendly Version

Interactive Discussion

5 triads are further distributed around each measured point, on a cubic grid centered on that point. The initial separations determining the size of the cube are 10 m in the vertical and 2500 m in the horizontal (based on the typical stratospheric aspect ratio of stratospheric tracer layers, Haynes and Anglade, 1997). Renormalization of the triad is performed every 24 h according to the standard algorithm of Benettin et al. (1980) and the Lyapunov exponents are averaged over the cube surrounding each point.

Influence of long range transport is seen as strong gradients and peaks in reconstructed mixing ratio profiles of tracers. Strong strain is represented by peaks in the Lyapunov exponents.

10 The first panel in Fig. 10 shows the exponents for SF2 flight focusing on the vertical range of the extra tropical tropical intrusion. The peaks at 16.5 km and slightly below 17 km mark regions of high stretching where gradients intensify orthogonally to the stretching direction. They mark the boundaries of the intrusion, where two backward trajectories separate rapidly. Conversely, the minima correspond to regions of the flow with small separation rates of back trajectories. These are associated with the core of the intrusion, where dispersion is small as suggested from Fig. 5.

The second panel of Fig. 10 shows two different diffusive reconstructions of O₃ mixing ratio along the same flight track, corresponding to diffusivities of 0.1 and 0.5 m² s⁻¹ compared to the measured profile, showing that the location of largest gradient agrees very well the peaks in the Lyapunov exponent. Therefore, the surfaces limiting the intrusion (above and below) where the contact is established between air masses coming from different origins can be considered as dynamical boundaries. This is further demonstrated in the third panel of Fig. 10 which shows the reconstruction from a non diffusive cloud of points initialized around each parcel at the points used for Lyapunov exponent calculation. It is clear that gradients reconstructed in that way are unrealistic, but it is striking to find that the boundary of the high O₃ region corresponds sharply to the peaks of the Lyapunov exponents.

25 Over the altitude range of the intrusion, one Lyapunov exponent is negative while the two others are positive with about the same magnitude. This indicates that stirring

generates filaments in the negative time and pancakes or sheets in the positive time.

4 Conclusions

We have shown that laminated structures in the O_3 profile found during the subtropical Hibiscus campaign can be identified with a long-range extratropical intrusion associated with breaking Rossby waves across the subtropical barrier. This intrusion carries air that trajectories trace back to polar latitudes less than 10 days before.

The peaks in the O_3 profile induced by extra-tropical intrusions are very well reconstructed during the active phase of the intrusion, when the large scale flow induces a clear separation between air masses. The reconstruction performs less well during the subsequent aging stage when unmixed extratropical air is preserved as sloping sheets in the subtropics and when separation relies on mesoscale stirring and mixing which is less constrained by data assimilation and hence less predictable. However, even in that case, reconstructed profiles in the vicinity of the balloon track reproduce ozone peaks with amplitude and vertical location close to the observations.

The best estimated value of Lagrangian turbulent diffusivity is $0.5 \text{ m}^2 \text{ s}^{-1}$ which is somewhat larger than that found at mid latitude in winter for the same levels ($0.1 \text{ m}^2 \text{ s}^{-1}$) (Legras et al., 2005).

The intrusion is fairly localized in altitude just above the level of the tropical tropopause and belongs to a range of altitude where meridional exchanges are favored (Vaugh, 1996).

The mid-height of the reconstructed intrusion does not vary with D . Both upper and lower edges and the maximum value are reconstructed with the same value of D while sharp peaks of stretching occur on the edges. This suggests that D cannot be solely related to local strain rate unlike the common assumption in most current parameterization and in agreement with previous findings at higher latitudes (Legras et al., 2005).

The generality of results found here is, however, somewhat limited by the scarcity of

Turbulent vertical diffusivity in the sub-tropical stratosphere

I. Pisso and B. Legras

Title Page

Abstract

Introduction

Conclusions

References

Tables

Figures

⏪

⏩

◀

▶

Back

Close

Full Screen / Esc

Printer-friendly Version

Interactive Discussion

the available dataset and clearly need to be confirmed by analysis of data from future campaigns.

Acknowledgements. We acknowledge the O3SSS team for the ozone data and G. Durry for H₂O and methane data. We acknowledge F. Lefèvre for the REPROBUS simulations and G. Berthet for fruitful discussions. I. Pisso was supported by a fellowship of the Ecole Polytechnique.

References

- Aliwell, S. R., Halsall, J. F., Pratt, K. F. E., O'Sullivan, J., Jones, R. L., Cox, R. A., Utembe, S. R., Hansford, G. M., and Williams, D. E.: Ozone sensors based on WO₃: a model for sensor drift and a measurement correction method, *Meas. Sci. Technol.*, 12, 684–690, 2001. [6606](#)
- Balluch, M. G. and Haynes, P. H.: Quantification of lower stratospheric mixing processes using aircraft data, *J. Geophys. Res.*, 102, 23 487–23 504, 1997. [6606](#)
- Benettin, G., Galgani, G., Giagilli, L., and Strelcyn, J.: Lyapunov characteristic exponents for smooth dynamical systems and for Hamiltonian systems; a method for computing all of them: I Theory, *Meccanica*, 15, 9–30, 1980. [6615](#)
- Del Castillo-Negrete, D. and Morrison, P.: Chaotic transport by Rossby waves in shear flow, *Phys. Fluids A: Fluid Dyn.*, 5(4), 948–965, 1993. [6604](#)
- Dexheimer, D. and Bowman, K.: Lagrangian methods for climatological analysis of regional atmospheric transport, *J. Appl. Meteorol.*, 43(4), 623–630, 2004. [6610](#)
- Hansford, G. M., Freshwater, R. A., Bosch, R. A., Cox, R. A., Jones, R. L., Pratt, K. F. E., and Williams, D. E.: A low cost instrument based on a solid state sensor for balloon-borne atmospheric O₃ profile sounding, *J. Environ. Monit.*, 7(2), 158–162, 2005. [6606](#)
- Haynes, P. H. and Anglade, J.: The vertical-scale cascade in atmospheric tracers due to large-scale differential advection, *J. Atmos. Sci.*, 54,9, 1112–1136, 1997. [6608](#), [6615](#)
- Haynes, P. H. and Shuckburgh, E.: Effective diffusivity as a diagnostic of atmospheric transport. Part II: troposphere and lower stratosphere, *J. Geophys. Res.*, 105(D18), 22 795–22 810, doi:10.1029/2000JD900092, 2000. [6604](#)
- Highwood, E. J. and Hoskins, B. J.: The tropical tropopause, *Q. J. R. Meteorol. Soc.*, 124(549), 1579–1604, 1998. [6604](#)

Turbulent vertical diffusivity in the sub-tropical stratosphere

I. Pisso and B. Legras

Title Page

Abstract

Introduction

Conclusions

References

Tables

Figures

⏪

⏩

◀

▶

Back

Close

Full Screen / Esc

Printer-friendly Version

Interactive Discussion

- Holton, J., Haynes, P. H., McIntyre, M., Douglass, A., Rood, R., and Pfister, L.: Stratosphere-troposphere exchange, *Rev. Geophys.*, 33(4), 403–439, 1995. [6605](#)
- Holzer, M. and Hall, T.: Transit-time and tracer-age distributions in geophysical flows, *J. Atmos. Sci.*, 57(21), 3539–3558, 2000. [6610](#)
- 5 Issartel, J.-P. and Baverel, J.: Inverse transport for the verification of the Comprehensive Nuclear Test Ban Treaty, *Atmos. Chem. Phys.*, 3, 475–486, 2003, <http://www.atmos-chem-phys.net/3/475/2003/>. [6610](#)
- Lefèvre, F., Brasseur, G. P., Folkins, I., Smith, A., and Simon, P.: Chemistry of the 1991-1992 stratospheric winter: Three dimensional model simulations, *J. Geophys. Res.*, 99, 8183–8195, 1994. [6610](#)
- 10 Lefèvre, F., Figarol, F., and ans T. Peter, K. C.: The 1997 Arctic ozone depletion quantified from three dimensional model simulations, *Geophys. Res. Lett.*, 25, 2425–2428, 1998. [6611](#)
- Legras, B., Pisso, I., Lefevre, F., and Berthet, G.: Variability of the Lagrangian turbulent diffusion in the lower stratosphere, *Atmos. Chem. Phys.*, 5, 1605–1622, 2005, <http://www.atmos-chem-phys.net/5/1605/2005/>. [6606](#), [6609](#), [6614](#), [6616](#)
- 15 McCormick, M. P. and Veiga, R. E.: Sagell Measurements of early Pinatubo aerosols, *Geophys. Res. Lett.*, 19, 155–158, 1992. [6605](#)
- Morse, P. and Feschbach, H.: *Methods of theoretical physics*, Mc-Graw-Hill, 1953. [6609](#)
- Neu, J. and Plumb, R.: Age of air in a “leaky pipe” model of stratospheric transport, *J. Geophys. Res.*, 104, 19 243–19 255, 1999. [6605](#)
- 20 Pierrehumbert, R. T. and Yang, H.: Global Chaotic Mixing on Isentropic Surfaces, *J. Atmos. Sci.*, 50, 2462–2480, 1993. [6605](#), [6614](#)
- Pommereau, J., Garnier, A., Held, G., Gomes, A.-M., Goutail, F., Durry, G., Borchì, F., Hauchecorne, A., Cocquerez, P., Letrenne, G., Vial, F., Hertzog, A., Legras, B., Pisso, I., Pyle, J. A., Harris, N. R. P., Jones, R. L., Robinson, A., Hansford, G., Eden, L., Gardiner, T., Swann, N., Knudsen, B., Larsen, N., Nielsen, J., Christensen, T., Cairo, F., Pirre, M., Marecal, V., Huret, N., Riviere, E., Coe, H., Grosvenor, D., Edvarsen, K., Donfrancesco, G. D., Ricaud, P., Longo, K., and Freitas, S.: An overview of the HIBISCUS campaign, *Atmos. Chem. Phys. Discuss.*, 7, 2389–2475, 2007, <http://www.atmos-chem-phys-discuss.net/7/2389/2007/>. [6606](#), [6607](#), [6612](#)
- 30 Stohl, A., Forster, C., Frank, A., and Wotawa, G.: Technical note: The Lagrangian particle dispersion model FLEXPART version 6.2, *Atmos. Chem. Phys.*, 5, 2461–2474, 2005, <http://www.atmos-chem-phys.net/5/2461/2005/>. [6610](#)

Turbulent vertical diffusivity in the sub-tropical stratosphereI. Pisso and B. Legras

Title Page

Abstract

Introduction

Conclusions

References

Tables

Figures

◀

▶

◀

▶

Back

Close

Full Screen / Esc

Printer-friendly Version

Interactive Discussion

Sudo, K., Takahashi, M., and Akimoto, H.: Future changes in stratosphere-troposphere exchange and their impacts on future tropospheric ozone simulations, *Geophys. Res. Lett.*, 30(24), 2256, 2003. [6605](#)

Waugh, D.: Seasonal variation of isentropic transport out of the tropical stratosphere, *J. Geophys. Res.*, 101(D2), 4007–4024, 1996. [6605](#), [6616](#)

Waugh, D. W. and Polvani, L.: Climatology of intrusions into the tropical upper troposphere, *Geophys. Res. Lett.*, 27 (23), 3857–3860, 2000. [6605](#)

Waugh, D. W., Plumb, R. A., and Polvani, L. M.: Nonlinear, Barotropic Response to a Localized Topographic Forcing: Formation of a “Tropical Surf Zone” and Its Effect on Interhemispheric Propagation, *J. Atmos. Sci.*, 54(11), 1401–1416, 1994. [6605](#)

Williams, D. E., Aliwell, S. R., Pratt, K. F. E., Caruana, D. J., Jones, R. L., Cox, R. A., Hansford, G. M., and Halsall, J.: Modelling the response of a tungsten oxide semiconductor as a gas sensor for the measurement of ozone, *Meas. Sci. Technol.*, 13, 923–931, 2002. [6606](#)

Williamson, D. L.: Semi-Lagrangian moisture transport in the NMC spectral model, *Tellus*, 142A, 413–428, 1989. [6611](#)

Turbulent vertical diffusivity in the sub-tropical stratosphere

I. Pisso and B. Legras

Title Page

Abstract

Introduction

Conclusions

References

Tables

Figures

◀

▶

◀

▶

Back

Close

Full Screen / Esc

Printer-friendly Version

Interactive Discussion

**Turbulent vertical
diffusivity in the
sub-tropical
stratosphere**

I. Pisso and B. Legras

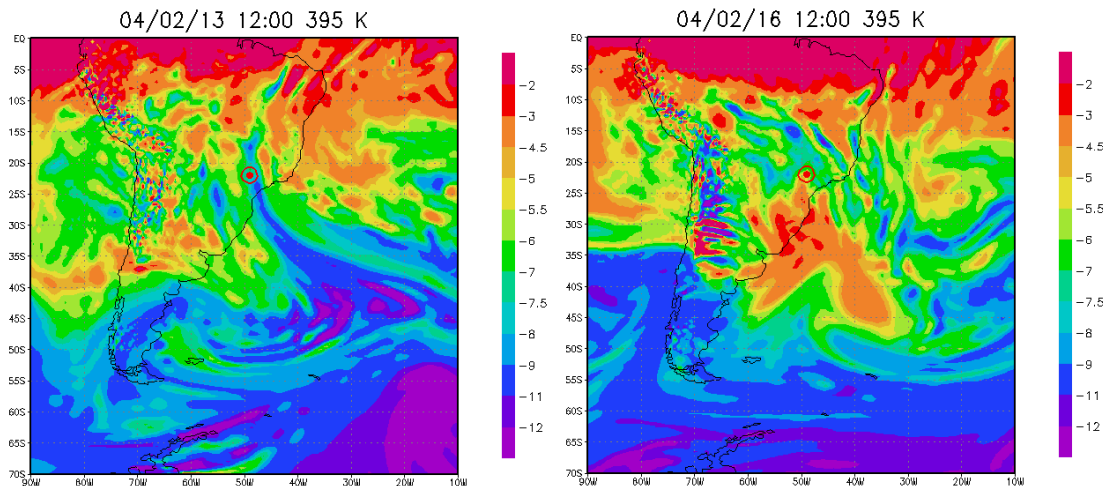


Fig. 1. Potential vorticity maps at $\theta=395$ K from ECMWF analysis over south-America and south-Atlantic. Left panel shows the meteorological situation on 13 February 2004 at 12:00 UT and right panel corresponds to 16 February 2004 at 12:00 UT. Units are in $\text{PVU}=10^6 \text{ m}^2 \text{ K s}^{-1} \text{ kg}^{-1}$. The launching site at Baru is circled in red.

[Title Page](#)[Abstract](#)[Introduction](#)[Conclusions](#)[References](#)[Tables](#)[Figures](#)[⏪](#)[⏩](#)[◀](#)[▶](#)[Back](#)[Close](#)[Full Screen / Esc](#)[Printer-friendly Version](#)[Interactive Discussion](#)

**Turbulent vertical
diffusivity in the
sub-tropical
stratosphere**

I. Pisso and B. Legras

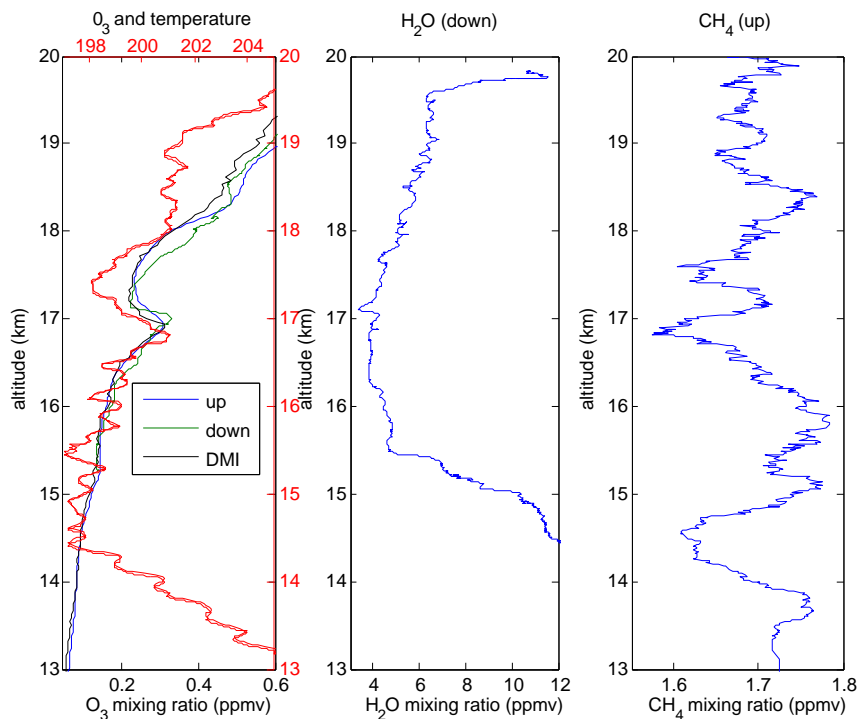


Fig. 2. The first panel compares O₃ profiles obtained during ascent (blue) and descent (green) of the SF2 flight on 13 February 2004 with temperature profile (red) collected during the same flight and O₃ profile measured by DMI ozonesonde. Second panel shows water vapor collected during SF2 descent and third panel shows methane collected during SF2 ascent. SF2 balloon was launched at 20:19 UT on 13 February. DMI ozonesonde was launched at 22:35 UT the same day.

[Title Page](#)[Abstract](#)[Introduction](#)[Conclusions](#)[References](#)[Tables](#)[Figures](#)[◀](#)[▶](#)[◀](#)[▶](#)[Back](#)[Close](#)[Full Screen / Esc](#)[Printer-friendly Version](#)[Interactive Discussion](#)

February 16, 2004

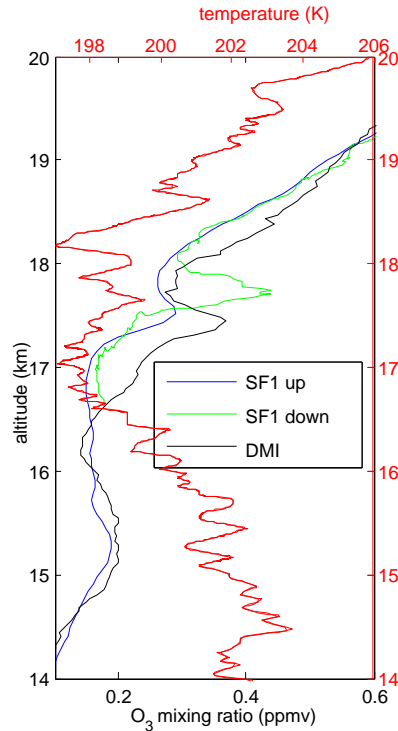


Fig. 3. Comparison of O₃ profiles obtained during ascent and descent of the SF1 flight on 16 February 2004 (blue) and DMI sonde the same day (green). Red curve represents temperature profile corresponding to SF1 flight. SF1 balloon was launched at 20:24 UT on 16 February. DMI ozonesonde was launched at 00:08 UT the same day.

ACPD

7, 6603–6629, 2007

Turbulent vertical diffusivity in the sub-tropical stratosphere

I. Pisso and B. Legras

Title Page

Abstract

Introduction

Conclusions

References

Tables

Figures

◀

▶

◀

▶

Back

Close

Full Screen / Esc

Printer-friendly Version

Interactive Discussion

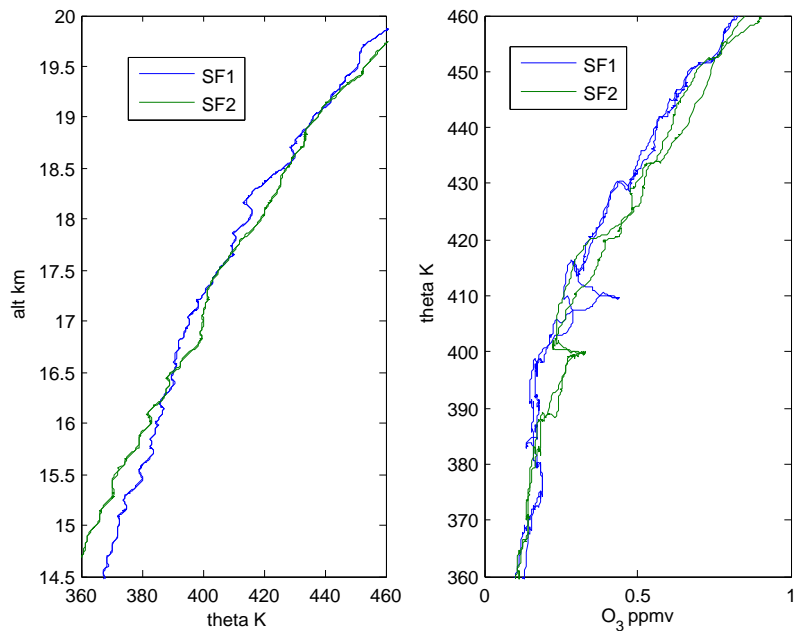


Fig. 4. Potential temperature θ as a function of altitude and O_3 mixing ratio as a function of θ for SF1 and SF2 flights, for both ascent and descent.

Turbulent vertical diffusivity in the sub-tropical stratosphere

I. Pisso and B. Legras

Title Page

Abstract

Introduction

Conclusions

References

Tables

Figures

◀

▶

◀

▶

Back

Close

Full Screen / Esc

Printer-friendly Version

Interactive Discussion

**Turbulent vertical
diffusivity in the
sub-tropical
stratosphere**

I. Pisso and B. Legras

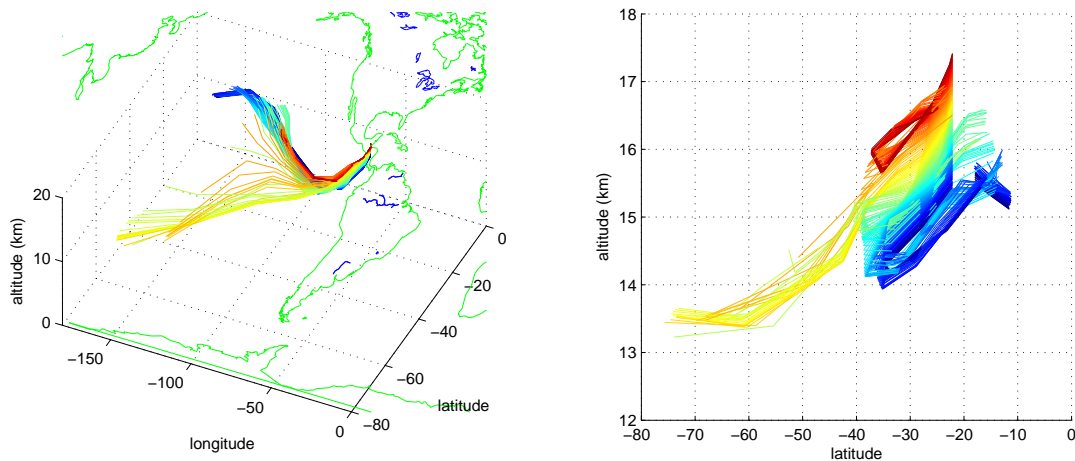


Fig. 5. Back trajectories initialized along SF2 balloon track and calculated over 9 days. Left panel: three dimensional representation. Right panel: projection on the vertical-meridional axis. Color code shows the altitude of the initial point of the trajectory.

[Title Page](#)[Abstract](#)[Introduction](#)[Conclusions](#)[References](#)[Tables](#)[Figures](#)[◀](#)[▶](#)[◀](#)[▶](#)[Back](#)[Close](#)[Full Screen / Esc](#)[Printer-friendly Version](#)[Interactive Discussion](#)

**Turbulent vertical
diffusivity in the
sub-tropical
stratosphere**

I. Pisso and B. Legras

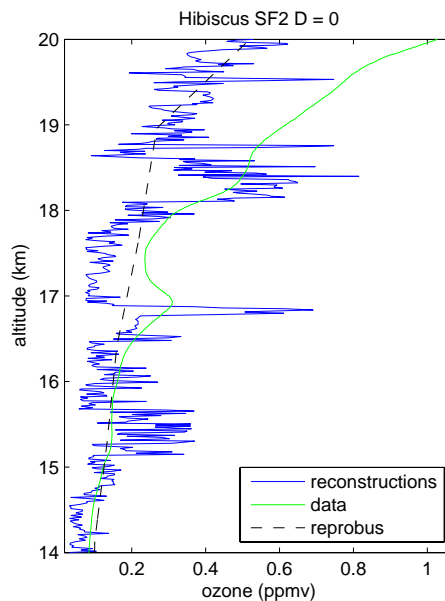


Fig. 6. Derministic reconstruction of SF2 ozone profile without diffusion. Each measurement point is represented by one trajectory. Vertical axis is the altitude along the balloon track. The green curve represents the ozone profile measured by SF2 flight. Lagrangian reconstructions without diffusion (in blue) are much rougher than measured profiles. The black dashed line shows the O_3 mixing ratios interpolated from global REPROBUS chemical fields on measurement locations.

[Title Page](#)[Abstract](#)[Introduction](#)[Conclusions](#)[References](#)[Tables](#)[Figures](#)[◀](#)[▶](#)[◀](#)[▶](#)[Back](#)[Close](#)[Full Screen / Esc](#)[Printer-friendly Version](#)[Interactive Discussion](#)

Turbulent vertical diffusivity in the sub-tropical stratosphere

I. Pisso and B. Legras

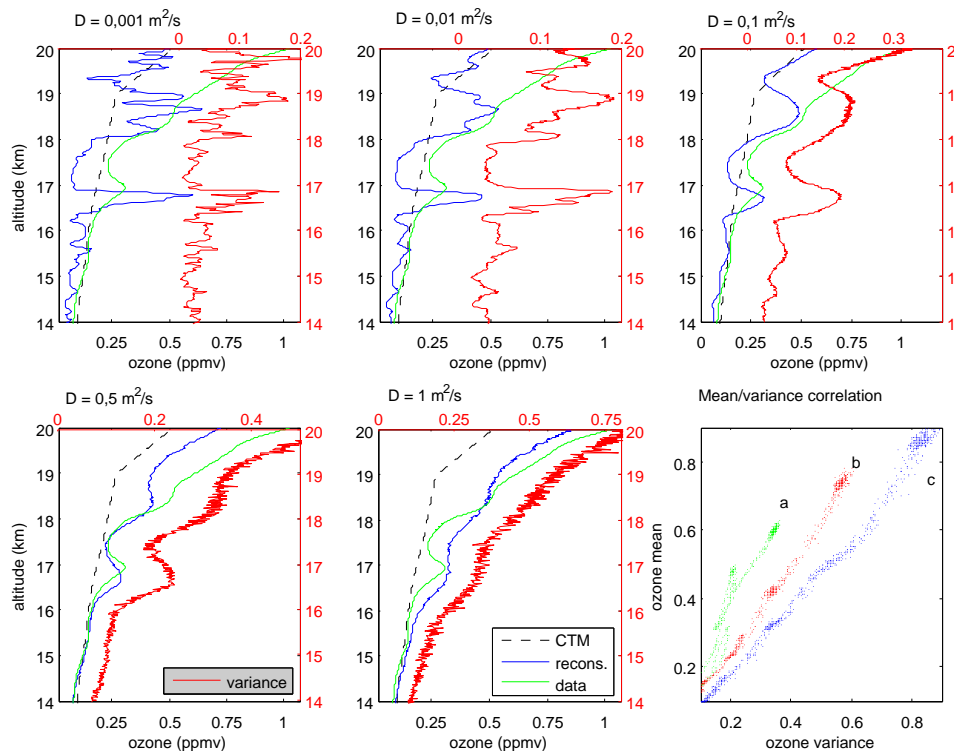


Fig. 7. Blue curves show diffusive reconstructions of SF2 ozone profile for values of D ranging from $10^{-3} \text{ m}^2 \text{ s}^{-1}$ (upper left panel) to $1 \text{ m}^2 \text{ s}^{-1}$ (lower center panel). Vertical axis is the altitude of initialization points. Green curves represent the ozone profile measured by SF2 flight and black dashed lines show the O₃ mixing ratios interpolated from global 3-D REPROBUS chemical fields. Red curves show the variance of O₃ mixing ratio associated with each individual cloud of trajectories. Values are read from the upper horizontal axis. Lower right panel shows the mean/variance correlation for the diffusive reconstructions along SF2 profile calculated for values of diffusivity of $0.1 \text{ m}^2 \text{ s}^{-1}$ (a), $0.5 \text{ m}^2 \text{ s}^{-1}$ (b) and $1 \text{ m}^2 \text{ s}^{-1}$ (c).

[Title Page](#)
[Abstract](#)
[Introduction](#)
[Conclusions](#)
[References](#)
[Tables](#)
[Figures](#)
[◀](#)
[▶](#)
[◀](#)
[▶](#)
[Back](#)
[Close](#)
[Full Screen / Esc](#)
[Printer-friendly Version](#)
[Interactive Discussion](#)

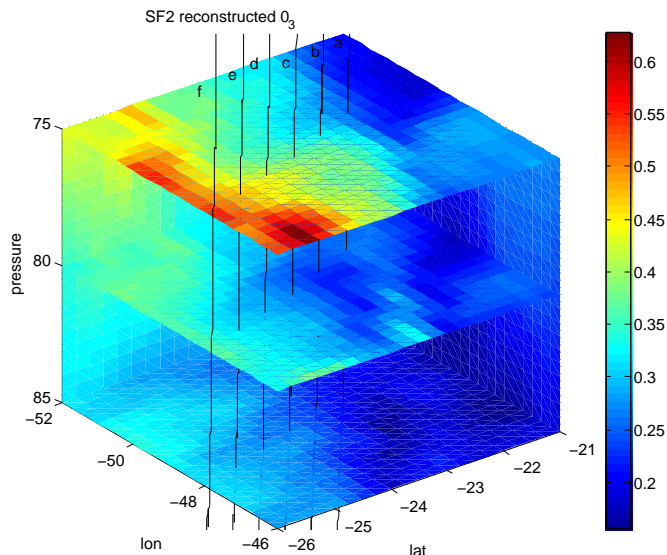


Fig. 8. Three dimensional distribution of O₃ in a neighborhood of the segment supporting the peak on 16 February. The region considered corresponds to three pressure levels (85, 80 and 75 hPa) from 21 S to 26 S in latitude and 46 W to 52 W in longitude. Ensembles of diffusive backward trajectories with a value of D of $0.1 \text{ m}^2 \text{ s}^{-1}$ were used to reconstruct the O₃ mixing ratio in a 1.5° horizontal grid and the result was interpolated on a 0.25° horizontal grid. The vertical lines represent the actual and shifted balloon tracks used to produce Fig. 9. A region of low O₃ is apparent at the level 80 hPa over the launching site. Color code represents O₃ mixing ratio in ppbv.

Turbulent vertical diffusivity in the sub-tropical stratosphere

I. Pisso and B. Legras

Title Page

Abstract

Introduction

Conclusions

References

Tables

Figures

◀

▶

◀

▶

Back

Close

Full Screen / Esc

Printer-friendly Version

Interactive Discussion

**Turbulent vertical
diffusivity in the
sub-tropical
stratosphere**

I. Pisso and B. Legras

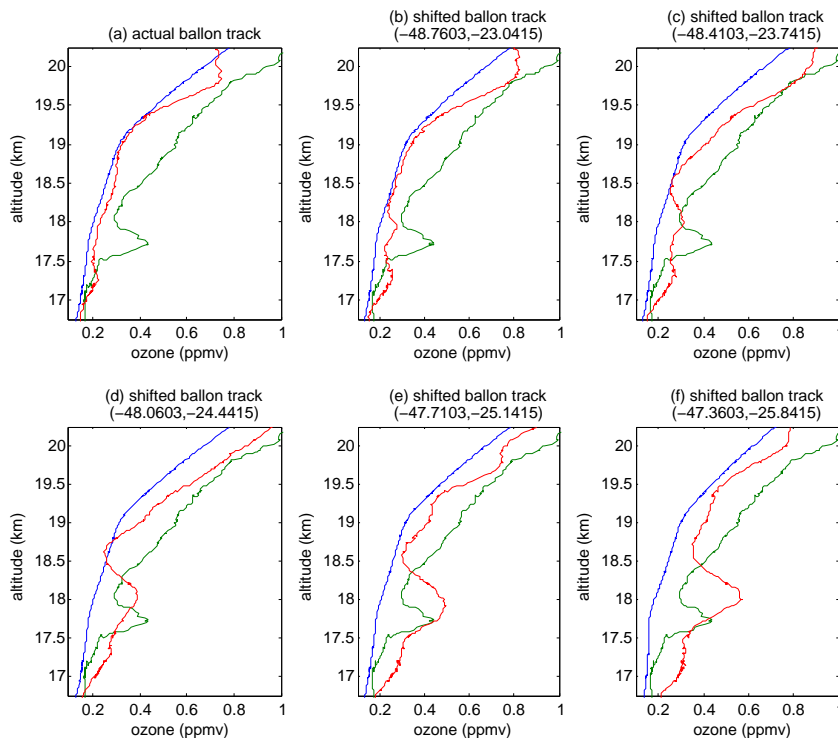


Fig. 9. O_3 diffusive reconstructions for the SF1 flight on 16 February 2004 (descent) performed with a diffusivity of $0.1 \text{ m}^2 \text{ s}^{-1}$. Upper left panel corresponds to the actual flight track, over the launching site at (49.03 W, 22.36 S). The following panels show diffusive reconstructions initialized by shifting the actual balloon track along a line running from the launch site to where reconstructed O_3 is high. A peak is observed in the lower three panels.

Title Page

Abstract

Introduction

Conclusions

References

Tables

Figures

◀

▶

◀

▶

Back

Close

Full Screen / Esc

Printer-friendly Version

Interactive Discussion

Turbulent vertical diffusivity in the sub-tropical stratosphere

I. Pizzo and B. Legras

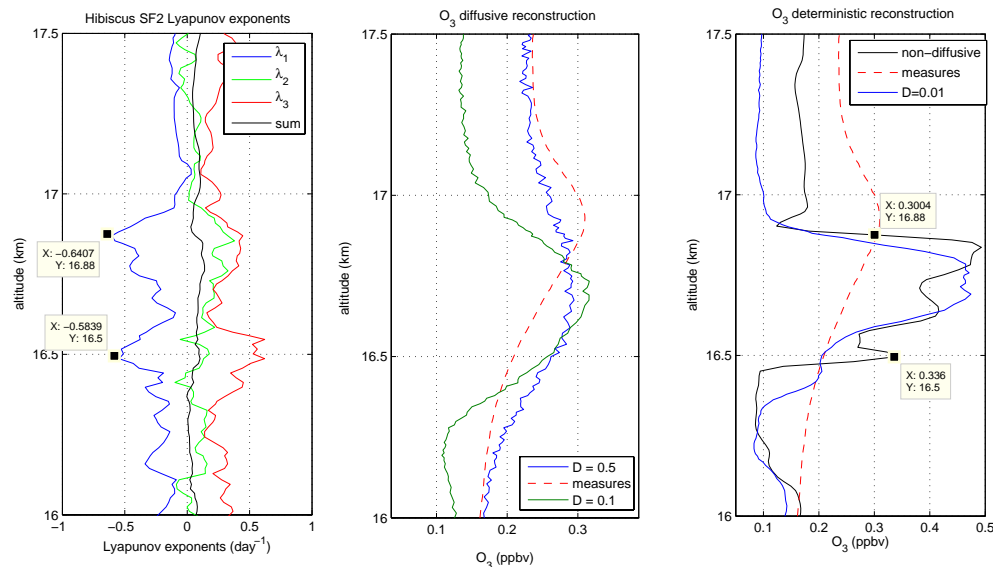


Fig. 10. Left panel: Three-dimensional Lyapunov exponents along SF2 balloon track. Blue curves show the largest rate of separation between two points for negative time (contraction in the positive time direction). Red curve shows the largest positive exponent, corresponding to contraction in negative time. Green curve shows the second exponent, which can be positive or negative. Black curve is the sum of the three exponents that should vanish for strictly incompressible flow but here slightly differs from zero due to compressibility and numerical errors. Center panel: diffusive reconstructions of O_3 mixing ratio. Right panel: weakly diffusive and non-diffusive reconstructions of O_3 mixing ratio.

Title Page

Abstract

Introduction

Conclusions

References

Tables

Figures

◀

▶

◀

▶

Back

Close

Full Screen / Esc

Printer-friendly Version

Interactive Discussion